Symbolic-Numeric Algorithm for Solving the Problem of Quantum Tunneling of a Diatomic Molecule through Repulsive Barriers

Sergue Vinitsky[1], Alexander Gusev[1], Ochbadrakh Chuluunbaatar[1,2], Luong Le Hai[1,3], Andrzej Góźdź[4], Vladimir L. Derbov[5], and Pavel Krassovitskiy[6]

[1] Joint Institute for Nuclear Research, Dubna, Moscow Region, Russia
vinitsky@theor.jinr.ru
[2] National University of Mongolia, UlaanBaatar, Mongolia
[3] Belgorod State University, Belgorod, Russia
[4] Institute of Physics, Maria Curie-Skłodowska University, Lublin, Poland
[5] Saratov State University, Saratov, Russia
[6] Institute of Nuclear Physics, Almaty, Kazakhstan

Abstract. Symbolic-numeric algorithm for solving the boundary-value problems that describe the model of quantum tunneling of a diatomic molecule through repulsive barriers is described. Two boundary-value problems (BVPs) in Cartesian and polar coordinates are formulated and reduced to 1D BVPs for different systems of coupled second-order differential equations (SCSODEs) that contain potential matrix elements with different asymptotic behavior. A symbolic algorithm implemented in CAS Maple to calculate the required asymptotic behavior of adiabatic basis, the potential matrix elements, and the fundamental solutions of the SCSODEs is elaborated. Comparative analysis of the potential matrix elements calculated in the Cartesian and polar coordinates is presented. Benchmark calculations of quantum tunneling of a diatomic molecule with the nuclei coupled by Morse potential through Gaussian barriers below dissociation threshold are carried out in Cartesian and polar coordinates using the finite element method, and the results are discussed.

Keywords: Symbolic-numeric algorithm, quantum tunneling problem, diatomic molecule, repulsive barriers, boundary-value problem, adiabatic representation, asymptotic solutions, finite element method.

1 Introduction

The study of tunneling of coupled particles through repulsive barriers [11] has revealed the effect of resonance quantum transparency: when the cluster size is comparable with the spatial width of the barrier, there are mechanisms that lead to greater transparency of the barrier. These mechanisms are related to the formation of the barrier resonances, provided that the potential energy of the composite system has local minima giving rise to metastable states of the moving cluster [10]. Currently this effect and its possible applications are a

V.P. Gerdt et al. (Eds.): CASC Workshop 2014, LNCS 8660, pp. 472–490, 2014.
© Springer International Publishing Switzerland 2014

subject of extensive study in relation with different quantum-physical problems, e.g., quantum diffusion of molecules [12], exciton resonance passage through a quantum heterostructure barrier [8], resonant formation of molecules from individual atoms [13], controlling the direction of diffusion in solids [1], and tunnelling of ions and clusters through repulsive barriers [7,6]. For the analysis of these effects, it is useful to develop model approaches based on approximations providing a realistic description of interactions between the atoms in the molecule as well as with the barriers, and to elaborate symbolic-numeric algorithms and software.

In this paper, we formulate and study the model of a diatomic molecule with the nuclei coupled via the effective Morse potential that penetrates through a Gaussian repulsive barrier, using Galerkin and Kantorovich expansion of the desired solution in Cartesian and polar coordinates, respectively. We formulate two boundary-value problems (BVP) and use different sets of basis functions to reduce the original problem to 1D BVPs for different systems of coupled second-order differential equations (SCSODEs) that contain potential matrix elements with different asymptotic behavior. In the first case, the potential matrix elements decrease exponentially, and in the second case, they decrease as inverse powers of the independent variable. In the second case, we must calculate the asymptotic behavior of the potential matrix elements to solve the boundary value problem. For this goal, we develop symbolic algorithms implemented in CAS Maple to calculate the required asymptotic behavior of the potential matrix elements as well as the fundamental solutions of SCSODEs. We present a comparative analysis of the potential matrix elements calculated in the Cartesian and polar coordinates, which are used to solve the quantum tunneling problem below the dissociation threshold. The necessity for two statements of the problem follows from the important practical applications of further self-consistent study of the system above the dissociation threshold, which is convenient in polar coordinates. The effect of quantum transparency, i.e., the resonance behavior of the transmission coefficient versus the energy of the molecule is analyzed.

The paper is organized as follows. In Sections 2 and 3, we formulate and solve the BVPs in Cartesian and polar coordinates. In Section 4, the leading terms of the asymptotic expressions of effective potentials and fundamental solutions are calculated using the elaborated algorithms in CAS Maple. In Section 5, we analyze the solution of the quantum tunneling problem below the dissociation threshold. In Conclusion, the prospects of future studies are discussed.

2 Model I. Quantum Tunneling in Cartesian Coordinates

We consider a 2D model of two identical particles with the mass m coupled by the pair potential $\tilde{V}(x_2 - x_1)$ and interacting with the external barrier potentials $\tilde{V}^b(x_1)$ and $\tilde{V}^b(x_2)$. Using the change of variables $x = x_2 - x_1$, $y = x_2 + x_1$,

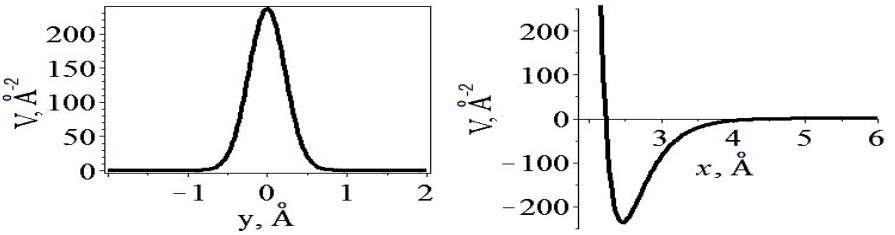

Fig. 1. Gaussian-type barrier $V^b(x_i) = \hat{D}\exp\left(-\frac{x_i^2}{2\sigma}\right)$, at $\hat{D} = 236.510003758401\text{Å}^{-2} = (m/\hbar^2)\tilde{V}_0 = (m/\hbar^2)D$, $\tilde{V}_0 = D = 1280\text{K}$, $\sigma = 5.23 \cdot 10^{-2}\text{Å}^2$, and the two-particle interaction potential, $V^M(x) = \hat{D}\{\exp[-2(x-\hat{x}_{eq})\hat{\rho}] - 2\exp[-(x-\hat{x}_{eq})\hat{\rho}]\}$, $\hat{x}_{eq} = 2.47\text{Å}$, $\hat{\rho} = 2.96812423381643\text{Å}^{-1}$

$y \in (-\infty, \infty)$, $x \in (-\infty, \infty)$, we arrive at the Schrödinger equation for the wave function $\Psi(x, y)$ in the s-wave approximation

$$\left(-\frac{\hbar^2}{m}\frac{1}{f_1(y)}\frac{\partial}{\partial y}f_2(y)\frac{\partial}{\partial y} - \frac{\hbar^2}{m}\frac{1}{f_3(x)}\frac{\partial}{\partial x}f_4(x)\frac{\partial}{\partial x} + \tilde{V}(x,y) - \tilde{E}\right)\Psi(y,x) = 0. \quad (1)$$

where $\hbar$ is the Planck constant, $\tilde{E}$ is the total energy of the system, and the potential function $V(x, y)$ is defined by the formula

$$\tilde{V}(x,y) = \tilde{V}^M(x) + \tilde{V}^b(x_1) + \tilde{V}^b(x_2). \quad (2)$$

The equation describing the molecular subsystem has the form

$$\left(-\frac{\hbar^2}{m}\frac{1}{f_3(x)}\frac{\partial}{\partial x}f_4(x)\frac{\partial}{\partial x} + \tilde{V}^M(x) - \tilde{\varepsilon}\right)\phi(x) = 0. \quad (3)$$

The molecular subsystem is assumed to possess the continuous energy spectrum with the eigenvalues $\tilde{\varepsilon} \geq 0$ and eigenfunctions $\phi_{\tilde{\varepsilon}}(x)$ and the discrete energy spectrum, consisting of the finite number n of bound states with the eigenfunctions $\phi_j(x)$ and the eigenvalues $\tilde{\varepsilon}_j = -|\tilde{\varepsilon}_j|$, $j = 1, n$.

The asymptotic boundary conditions imposed on the solution for the 2D model in the s-wave approximation $\Psi(y, x) = \{\Psi_j(y, x)\}_{j=1}^{N_o}$ in the asymptotic region $\Omega_j^{as} = \{(x, y)||x|/|y| \ll 1\}$ with the direction $v = \rightarrow$ can be written in the obvious form

$$\begin{aligned}
&\Psi_j(y \to -\infty, x) \to \phi_j(x)\frac{\exp(\imath p_j y)}{\sqrt{p_j f_2(y)}} + \sum_{l=1}^{N_o}\phi_l(x)\frac{\exp(-\imath p_l y)}{\sqrt{p_l f_2(y)}}R_{lj},\\
&\Psi_j(y \to +\infty, x) \to \sum_{l=1}^{N_o}\phi_l(x)\frac{\exp(\imath p_l y)}{\sqrt{p_l f_2(y)}}T_{lj},\\
&\Psi_j(y, x \to \pm\infty) \to 0,
\end{aligned} \quad (4)$$

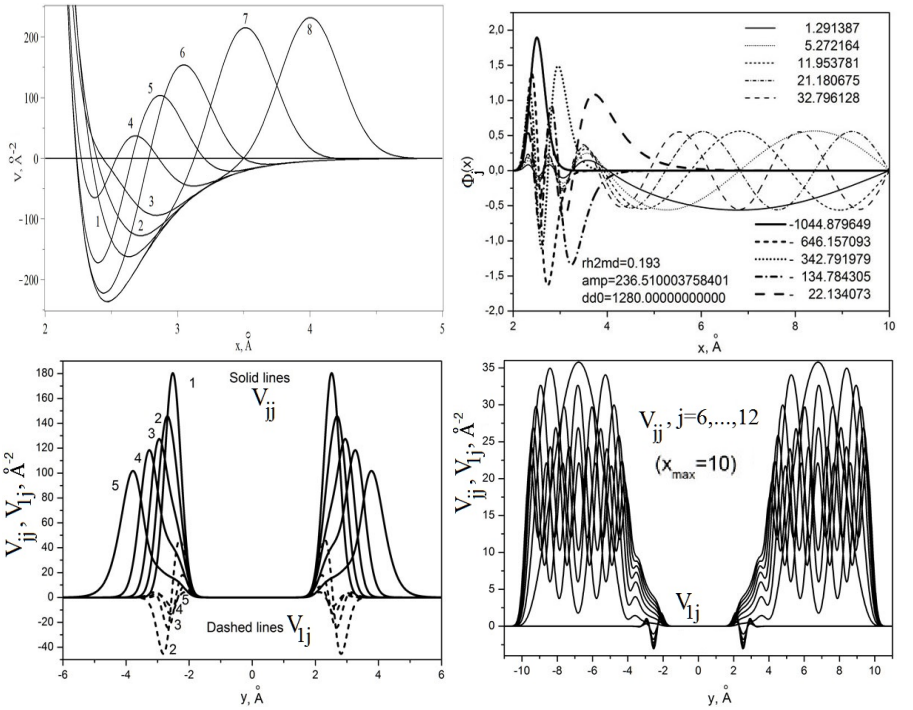

Fig. 2. Sections of the total potential energy $V(y;x) = V^M(y;x) + V^b(y;x)$ at $y = 2.2, 2.3, 2.4, 2.6, 2.8, 3, 3.5, 4$ (curves are noted by 1,...,8). The wave functions $\phi_j(r)$ of the bound states $j = 1, 5$ (solid lines) and pseudostates $j = 6, ..., 12$ (dashed lines) (corresponding energy eigenvalues given in K). The matrix elements $V_{jj}(y)$ (solid lines) and $V_{j1}(y)$ (dashed lines) (in $\mathring{A}^{-2}$)

where $f_1(y) = f_2(y) = 1$, $R_{lj}(\tilde{E})$ and $T_{lj}(\tilde{E})$ are the reflection and transmission amplitudes, $N_o \leq n$ is the number of open channels, p_i is the wave number, $p_i = \sqrt{(m/\hbar^2)(\tilde{E} - \tilde{\varepsilon}_i)} > 0$, below dissociation threshold $\tilde{E} < 0$, $\phi_j(x)$ and $\varepsilon_j < 0$ at $j = 1, n$ are the eigenfunctions and eigenvalues of the BVP for Eq. (3).

The solution of Eq. (1) is sought for in the form of Galerkin expansion

$$\Psi_{i_o}(y, x) = \sum_{j=1}^{j_{\max}} \phi_j(x)\chi_{ji_o}(y). \tag{5}$$

Here $\chi_{ji_o}(y)$ are unknown functions and the orthonormalized basis functions $\phi_j(x)$ in the interval $0 \leq x \leq x_{\max}$ are defined as eigenfunctions of the BVP for the equation

$$\left(-\frac{1}{f_3(x)}\frac{\partial}{\partial x}f_4(x)\frac{\partial}{\partial x} + V^M(x) - \varepsilon_j\right)\phi_j(x) = 0, \tag{6}$$

with the boundary and orthonormalization conditions

$$\phi_j(0) = \phi_j(x_{\max}) = 0, \quad \int_0^{x_{\max}} f_3(x)dr\phi_i(x)\phi_j(x) = \delta_{ij}, \tag{7}$$

where $f_3(x) = f_4(x) = 1$, $V(x) = (m/\hbar^2)\tilde{V}(x)$, $\varepsilon_j = (m/\hbar^2)\tilde{\varepsilon}_j$. The desired set of numerical solutions of this BVP is calculated with the given accuracy by means of the program ODPEVP [4]. Hence, we calculate the set of n bound states having the eigenfunctions $\phi_j(x)$ and the eigenvalues ε_j, $j = 1, n$ and the desired set of pseudostates with the eigenfunctions $\phi_j(x)$ and the eigenvalues $\varepsilon_j \geq 0$, $j = n+1, j_{\max}$. The latter approximate the set of continuum eigensolutions $\varepsilon \geq 0$ of the BVP for Eq. (3).

The set of closed-channel Galerkin equations has the form

$$\left[-\frac{1}{f_1(y)}\frac{\partial}{\partial y}f_2(y)\frac{\partial}{\partial y} + \varepsilon_i - E\right]\chi_{ii_o}(y) + \sum_{j=1}^{j_{\max}} V_{ij}^b(y)\chi_{ji_o}(y) = 0. \tag{8}$$

Thus, the scattering problem (1)–(3) with the asymptotic boundary conditions (4) is reduced to the boundary-value problem for the set of close-coupling equations in the Galerkin form (8) for $f_1(y) = f_2(y) = 1$ with the boundary conditions at $y = y_{\min}$ and $y = y_{\max}$ [6]:

$$\left.\frac{d\boldsymbol{F}(y)}{dy}\right|_{y=y_t} = \mathcal{R}(y_t)\boldsymbol{F}(y_t), \quad t = \min, \max, \tag{9}$$

where $\mathcal{R}(y_{\min})$ and $\mathcal{R}(y_{\max})$ are $j_{\max} \times j_{\max}$ symmetric matrix function of E, $\boldsymbol{F}(y) = \{\boldsymbol{\chi}_{i_o}(y)\}_{i_o=1}^{N_o} = \{\{\chi_{ji_o}(y)\}_{j=1}^{j_{\max}}\}_{i_o=1}^{N_o}$ is the required $j_{\max} \times N_o$ matrix solution at the number of open channels $N_o = \max_{E \geq \varepsilon_j} j \leq j_{\max}$. These matrices and the sought-for $N_o \times N_o$ matrices of the reflection and transmission amplitudes $\mathbf{R}$ and $\mathbf{T}$ are calculated using the third version of the program KANTBP [3].

In Eq. (8), the effective potentials $V_{ij}(y)$ are expressed by the integrals

$$V_{ij}^b(y) = \int_0^{x_{\max}} f_1(x)dx\phi_i(x)(V^b(\frac{x+y}{2}) + V^b(\frac{x-y}{2}))\phi_j(x). \tag{10}$$

For example, let us take the parameters of the molecule Be_2, namely, the reduced mass $\mu = m/2 = 4.506$Da, the average distance between the nuclei 2.47Å, the frequency of molecular vibrations expressed in temperature units $\hbar\omega = 398.72$K, the ground state of molecule $^1\Sigma_u^+$, the wave number of the order of 277.124cm^{-1} for the observable excited-to-ground state transitions (we use the relation $1\text{K} = 0.69503476\ \text{cm}^{-1}$ from [5]). These values were used to determine the parameters of the Morse potential $\tilde{V}^M(x)$ and $V^M(x) = (m/\hbar^2)\tilde{V}^M(x)$ of Eqs. (3) and (6)

$$\tilde{V}^M(x) = D\{\exp[-2(x - \hat{x}_{eq})\hat{\rho}] - 2\exp[-(x - \hat{x}_{eq})\hat{\rho}]\}, \tag{11}$$

where D is the depth of the interaction potential well and $\hat{\rho}$ describes the potential well width. The values of D and $\hat{\rho}$ are determined from the discrete spectrum

of the BVP (6)–(7) which is approximated by the known discrete spectrum of Eq. (3)

$$\tilde{\varepsilon}_j = -D\left[1 - \varsigma(j - 1/2)\right]^2, \quad j = 1, ..., n = \left[\varsigma^{-1} + \frac{1}{2}\right]. \tag{12}$$

The discrete spectrum eigenfunctions $\phi_j(x)$ of the BVP (6)–(7) are approximated by the solutions $\tilde{\phi}_j(\zeta)$ of equation (3) in the new variable ζ:

$$\frac{d^2\tilde{\phi}_j(\zeta)}{d\zeta^2} + \frac{1}{\zeta}\frac{d\tilde{\phi}_j(\zeta)}{d\zeta} + \left(-\frac{1}{4} + \frac{j + s_j - 1/2}{\zeta} - \frac{s_j^2}{\zeta^2}\right)\tilde{\phi}_j(\zeta) = 0,$$

where $s_j = \sqrt{-\varepsilon_j}/\hat{\rho} = \sqrt{\hat{D}}/\hat{\rho} - j + 1/2$ and $\zeta = 2\sqrt{\hat{D}}\exp[-(x - \hat{x}_{eq})\hat{\rho}]/\hat{\rho}$, at $\zeta \in (0, +\infty)$ corresponding to the extended interval $x \in (-\infty, +\infty)$ and have the form

$$\tilde{\phi}_j(\zeta) = N_j \exp(-\frac{\zeta}{2})\zeta^{s_j}{}_1F_1(1-j, 2s_j+1, \zeta),\ N_j^2 = \frac{\hat{\rho}\Gamma(2s_j+j)}{(j-1)!\Gamma(2s_j)\Gamma(2s_j+1)}. \tag{13}$$

Having the average size of the molecule and the separation between the energy levels taken into account, one can parameterize the molecular potential to fit the observable quantities, namely, $D = 1280\text{K}$, $\hat{x}_{eq} = 2.47\text{Å}$, $\hat{\rho} = 2.968\text{Å}^{-1}$ is determined from the condition $(\tilde{\varepsilon}_2 - \tilde{\varepsilon}_1)/(2\pi\hbar c) = 277.124\ \text{cm}^{-1}$, $\varsigma = \frac{\hat{\rho}\hbar}{\sqrt{mD}} = 0.193$ is the dimensionless constant of the problem, and $\hat{D} = (\frac{\sqrt{mD}}{\hbar})^2 = (\hat{\rho}/0.193)^2 = (2.968\text{Å}^{-1}/0.193)^2 = 236.5\text{Å}^{-2}$. In accordance with (12), the ground state energy of the molecule Be_2 is equal to $-\tilde{\varepsilon}_1 = -1044.88\text{K}$.

The set of pseudostates with the eigenfunctions $\phi_j(x)$ and the eigenvalues $\varepsilon_j \geq 0$, $j = n+1, j_{\max}$, approximated by the set of continuous spectrum solutions $\tilde{\phi}_k(\zeta)$ with fixed $k = \sqrt{\varepsilon} > 0$ that satisfy Eq. (3) written in the new variable ζ, i.e., the equation

$$\frac{d^2\tilde{\phi}_k(\zeta)}{d\zeta^2} + \frac{1}{\zeta}\frac{d\tilde{\phi}_k(\zeta)}{d\zeta} + \left(-\frac{1}{4} + \frac{\sqrt{\hat{D}}/\hat{\rho}}{\zeta} + \frac{s_k^2}{\zeta^2}\right)\tilde{\phi}_k(\zeta) = 0.$$

At fixed $s_k = \frac{k}{\hat{\rho}}$, these solutions take the form

$$\begin{aligned}\tilde{\phi}_k(\zeta) = \frac{N_k \exp(-\zeta/2)}{2i}&(\exp(iw)\zeta^{-ik/\hat{\rho}}{}_1F_1(-\frac{\sqrt{D}}{\hat{\rho}} + \frac{1}{2} - \frac{ik}{\hat{\rho}}, 1 - \frac{2ik}{\hat{\rho}}, \zeta)\\ &- \exp(-iw)\zeta^{ik/\hat{\rho}}{}_1F_1(-\frac{\sqrt{D}}{\hat{\rho}} + \frac{1}{2} + \frac{ik}{\hat{\rho}}, 1 + \frac{2ik}{\hat{\rho}}, \zeta)),\\ w = \arg(\Gamma(1 + \frac{2ik}{\hat{\rho}})) &+ \arg(\Gamma(-\frac{\sqrt{D}}{\hat{\rho}} + \frac{1}{2} - \frac{ik}{\hat{\rho}}))).\end{aligned} \tag{14}$$

Asymptotically $\tilde{\phi}_k^{as}(x \to \infty) = \sin(kx + \delta(k))$, $\delta(k) = -kx_{eq} - s_k \ln(2\sqrt{\hat{D}}/\hat{\rho}) + w$ corresponds to the scattering phase.

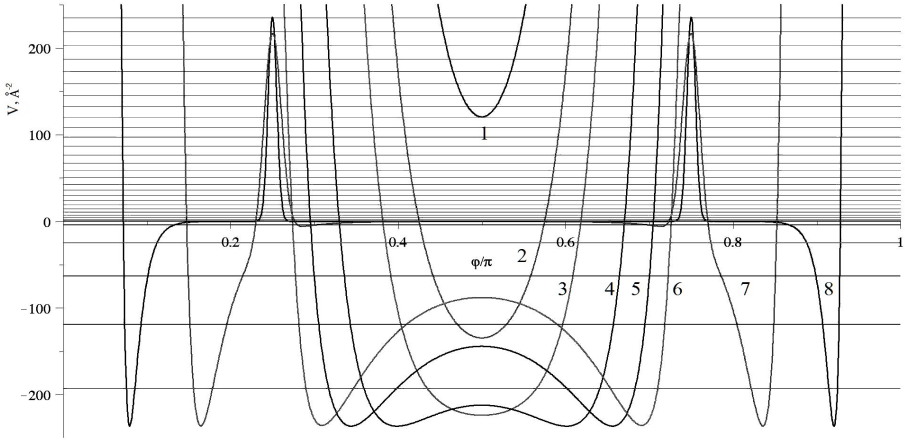

Fig. 3. Sections of the total potential energy $V(\rho;\varphi) = V^M(\rho;\varphi) + V^b(\rho;\varphi)$ in polar coordinates at $\rho = 2.2, 2.3, 2.4, 2.6, 2.8, 3, 5, 10$ (curves are noted by 1,...,8). Straight lines are energy levels at $\rho = 10$.

Since the bond in the molecule Be_2 is of the Van der Waals type, one can consider each constituent atom independently interacting with the external barrier potential. The latter should be chosen to have the height and the width typical of barriers in a real crystal lattice. Moreover, this potential should be a smooth function having the second derivative to apply high-accuracy numerical methods, like the Numerov method or the finite element method, for solving the BVP for the systems of second-order ordinary differential equations. We choose the repulsive barrier potential to be Gaussian:

$$\tilde{V}^b(x_i) = \tilde{V}_0 \exp\left(-\frac{x_i^2}{2\sigma}\right), \quad V^b(x_i) = \frac{m}{\hbar^2}\tilde{V}^b(x_i) = \hat{D}\exp\left(-\frac{x_i^2}{2\sigma}\right). \qquad (15)$$

Here the parameters $\tilde{V}_0 = 1280K$, $\hat{D} = 236.510003758401\text{Å}^{-2} = (m/\hbar^2)\tilde{V}_0$, $\sigma = 5.23 \cdot 10^{-2}\text{Å}^2$ are determined by the model requirement that the width of the repulsive potential at the kinetic energy equal to that of the ground state is 1Å, so that the average distance 2.47Å between the atoms of Be is smaller than the distance 2.56Å between Cu atoms in the plane (111) of the crystal lattice cell. The potential barrier height $\tilde{V}_0$ of the order of 200 meV was estimated following the experimental observation of quantum diffusion of hydrogen atoms [9]. Fig. 1 illustrates the Gaussian and Morse potentials.

Figure 2 presents the sections of the total potential energy, the calculated eigenfunctions of the BVP (6) and the effective potentials $V_{ij}(y)$ of Eq. (10) calculated using these functions. Note that the wave functions $\phi_j(x)$ and the eigenvalues $\varepsilon_j(x)$ of the bound states $j = 1, 5$ (solid lines) approximate the known analytical ones of the BVP for Eq. (3) with the Morse potential (11) with four and seven significant digits, respectively. The states are localized in the well,

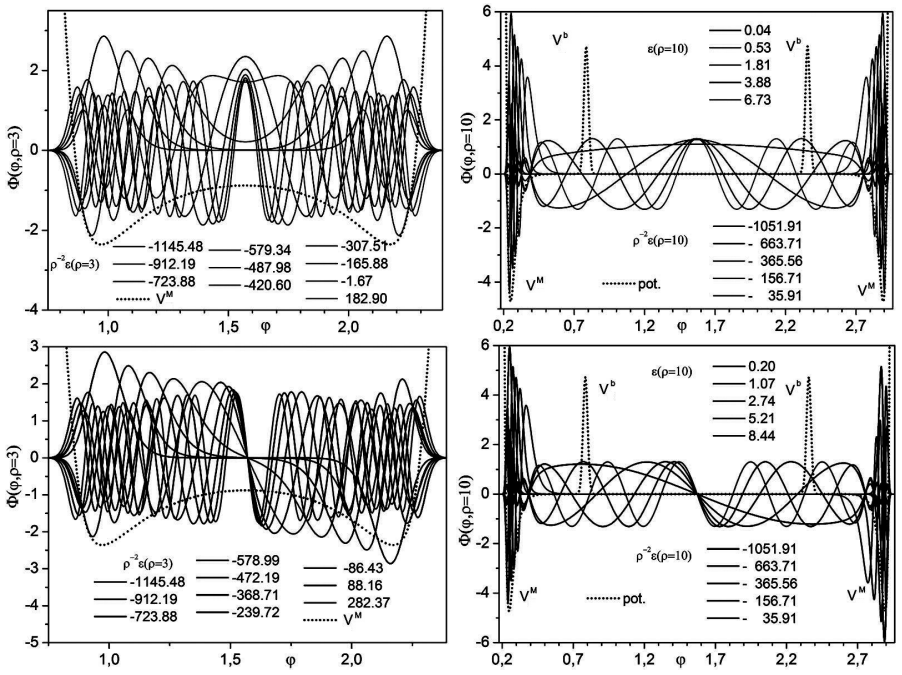

Fig. 4. Even and odd eigenfunctions of the parametric eigenvalue problem for the fast subsystem at $\rho = 3$ and $\rho = 10$ (corresponding energy eigenvalues given in K)

while the pseudostates $j = 6, ..., 12$ are approximated with the same accuracy and localized outside the well. The matrix elements between the bound states are localized in the vicinity of the barriers and the matrix elements between the pseudostates are localized beyond the barriers. The matrix elements between the bound states and pseudostates are small. The solution of the BVP (6), (7) was performed on the finite-element grids $\Omega_x = \{0(N_{elem} = 800)12\}$, with N_{elem} fourth-order Lagrange elements $p = 4$ between the nodes, using the program ODPEVP [4].

3 Model II. Quantum Tunneling in Polar Coordinates

Using the change of variables $x = \rho \sin\varphi$, $y = \rho \cos\varphi$, we can rewrite Eq. (1) in polar coordinates (ρ, φ) $\Omega_{\rho,\varphi} = (\rho \in (0, \infty), \varphi \in [0, \pi])$ in the dimensionless form

$$\left(-\frac{1}{\rho}\frac{d}{d\rho}\rho\frac{d}{d\rho} - \frac{1}{\rho^2}\frac{\partial^2}{\partial\varphi^2} + V(\rho,\varphi) - E\right)\Psi(\rho,\varphi) = 0, \tag{16}$$

where the potential function $V(\rho,\varphi) = V^M(\rho,\varphi) + V^b(\rho,\varphi)$ is defined by the formula in term of potentials (11) and (15)

$$V^M(\rho,\varphi)=V(\rho\sin\varphi),\ V^b(\rho,\varphi)=V^b(\rho\frac{\sin(\varphi+\pi/4)}{\sqrt{2}})+V^b(\rho\frac{\sin(\varphi-\pi/4)}{\sqrt{2}}). \quad (17)$$

Sections of the potential function $V(\rho,\varphi)$ at a set of slow variable values ρ are shown in Fig. 3. One can see that at large ρ, the width of the potential wells decreases as ρ increases. Therefore, at large ρ, the potential of two-center problem, symmetric with respect to $\varphi = \pi/2$, transforms into two one-center Morse potentials.

The asymptotic boundary conditions imposed on the solution for the 2D model in the s-wave approximation $\Psi(\rho,\varphi) = \{\Psi_j(\rho,\varphi)\}_{j=1}^{N_o}$ in the asymptotic region $\Omega_j^{as} = \{(\varphi,\rho)|\varphi/\rho \ll 1\}$ can be written in the obvious form

$$\Psi(\rho,\varphi,\varphi_0) = \sum_{i_o=1}^{N_o} \Psi_{ji_o}(\rho,\phi)\phi_{i_o}(-\varphi_0;\rho\to+\infty) \quad (18)$$

$$\Psi_{i_o}(\rho\to+\infty,\varphi) \to \sqrt{\frac{2}{\pi}}\sum_{j=1}^{N_o}\phi_j(\varphi;\rho)\left[\chi^*_{ji_o}(\rho)\delta_{ji_o} - \chi_{ji_o}(\rho)S_{ji_o}(E)\right], \quad (19)$$

$$\Psi_{i_o}(\rho,\phi\to 0)\to 0, \quad \Psi_{i_o}(\rho,\phi\to\pi)\to 0, \quad \chi_{ji_o}(\rho) = \frac{\exp(\imath(p_j\rho - \frac{\pi}{4}))}{2\sqrt{p_j\rho}},$$

where the angle φ_0 determines the direction of the incident wave propagation, in particular, $\varphi_0 = 0$ corresponds to $v =\rightarrow$ and $\varphi_0 = \pi$ corresponds to $v =\leftarrow$. $S_{ji_o}(E)$ are the elements of the $N_o \times N_o$ **S**-matrix, N_o is the number of open channels, p_i is the wave number, $p_i = \sqrt{(m/\hbar^2)(\tilde{E} - \tilde{\varepsilon}_i(\rho\to+\infty))} > 0$, below the dissociation threshold $\tilde{E} < 0$, $\phi_i(\varphi,\rho\to+\infty) = \sqrt{\rho}\phi_i(x)$, and $\varepsilon_i(\rho\to\infty)/\rho^2 = \varepsilon_i^{(0)} < 0$ are the eigenfunctions localized in the asymptotic region Ω_j^{as}, and the eigenvalues of the BVP for Eq. (21).

The solution of Eq. (16) is sought for in the form of Kantorovich expansion

$$\Psi_{i_o}(\rho,\varphi) = \sum_{j=1}^{j_{\max}}\phi_j(\varphi;\rho)\chi_{ji_o}(\rho). \quad (20)$$

Here $\chi_{ji_o}(\rho)$ are unknown functions and the orthonormalized basis functions $\phi_j(\varphi;\rho)$ in the interval $\varphi\in[0,\pi]$ are defined as eigenfunctions of the BVP for the equation

$$\left(-\frac{\partial^2}{\partial\varphi^2} + \rho^2(V^M(\rho\sin\varphi) + V^b(\rho,\phi)) - \varepsilon_j(\rho)\right)\phi_j(\varphi;\rho) = 0, \quad (21)$$

with orthonormalization conditions

$$\int_0^\pi d\varphi\phi_i(\varphi;\rho)\phi_j(\varphi;\rho) = \delta_{ij}. \quad (22)$$

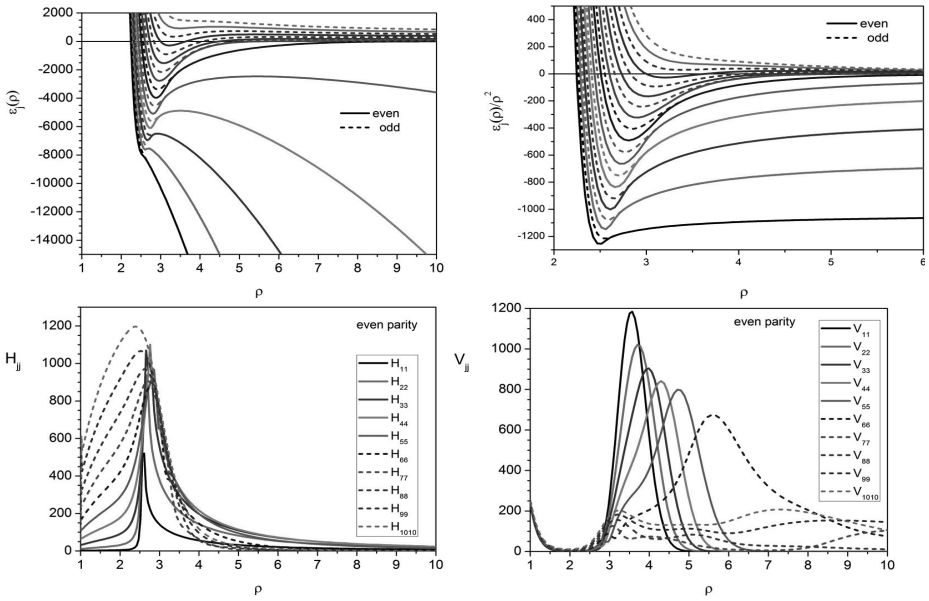

Fig. 5. Potential curves $\varepsilon_j(\rho)$ and even diagonal effective potentials $H_{jj}(\rho)$ and $V^b_{jj}(\rho)$ vs ρ (Å)

The solution of the BVPs (21), (22) was performed on the finite-element grids $\Omega_\varphi = \{\varphi_1(N_{elem} = 800)\pi/2\}$, if $\varphi_3 = (8+\varphi x_{eq})/(\varphi\rho) > \pi/4$, $\Omega_\varphi = \{\varphi_1(N_{elem} = 300)\varphi_2(N_{elem} = 60)\varphi_4(N_{elem} = 40)\varphi_5(N_{elem} = 100)\pi/2\}$ with N_{elem} fourth-order Lagrange elements $p = 4$ between the nodes, using the program ODPEVP [4]. Here angles $\varphi_1 = (-3 + \varphi x_{eq})/(\varphi\rho)$ and $\varphi_2 = (4 + \varphi x_{eq})/(\varphi\rho)$ are marked left and right bounds of well (17) and angles $\varphi_4 = \pi/4 - 4\sqrt{\sigma}/\rho$ and $\varphi_5 = \pi/4 + 4\sqrt{\sigma}/\rho$ are marked left and right bounds of potential barrier (17).

First, let us put $V^b(\rho, \varphi) = 0$ in Eq. (21). In this case, we calculate the set of n bound states having the eigenfunctions $\phi_j(\varphi; \rho)$ and the eigenvalues $\varepsilon_j(\rho) < 0$ at $j, = 1, 2, ..., n$, and the desired set of pseudostates with the eigenfunctions $\phi_j(\varphi; \rho)$ and the eigenvalues $\varepsilon_j(\rho) \geq 0$ at $j = n + 1, ..., j_{\max}$. The latter approximate the set of continuum eigensolutions $\varepsilon(\rho) \geq 0$ of the BVP for Eq. (3). The eigenvalues have the following asymptotes: $\varepsilon_j(\rho \to \infty)/\rho^2 = \varepsilon_j$ at $j, = 1, 2, ..., n$ and $\varepsilon_j(\rho \to \infty)/\rho^2 = (j - n)^2/\rho^2 + O(1/\rho^3)$ at $j = n + 1, ..., j_{\max}$.

The eigenfunctions $\phi_j(\varphi; \rho)$, $j = 1, 20$ are shown in Fig. 4 at $\rho = 3$ and $\rho = 10$. Taking the above symmetry $V(\varphi, \rho) = V(\pi - \varphi, \rho)$ of the potential into account, the eigenfunctions are separated into two subsets, namely, the even $\phi_j^{\sigma=1}(\varphi; \rho)$ and odd $\phi_j^{\sigma=-1}(\varphi; \rho)$ ones. The linear combinations

$$\phi_j^{\rightarrow\leftarrow}(\varphi; \rho) = (\phi_j^{\sigma=1}(\varphi; \rho) \pm \phi_j^{\sigma=-1}(\varphi; \rho))/\sqrt{2}$$

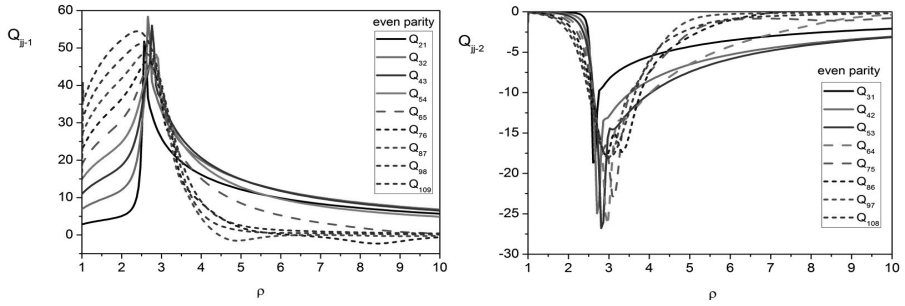

Fig. 6. Even effective potentials $Q_{ij}(\rho)$ vs ρ (Å)

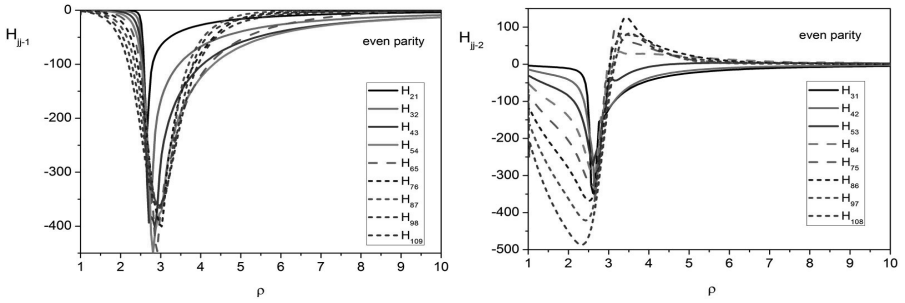

Fig. 7. Even effective potentials $H_{ij}(\rho)$ vs ρ (Å)

at large ρ have maxima in the vicinity of $\varphi = 0$ and $\varphi = \pi$, respectively, such that they correspond to the functions presented in Fig. 2. Taking this property into account, we arrive at the expressions [2]

$$\check{\mathbf{T}} = (-\check{\mathbf{S}}_{+1} + \check{\mathbf{S}}_{-1})/2, \quad \check{\mathbf{R}} = (-\check{\mathbf{S}}_{+1} - \check{\mathbf{S}}_{-1})/2, \tag{23}$$

which relate the even $\check{\mathbf{S}}_{+1}$ and odd $\check{\mathbf{S}}_{-1}$ elements of the matrix $\check{\mathbf{S}} = e^{\imath\pi/4}\mathbf{S}e^{\imath\pi/4}$ from Eq. (19) to the transmission $\check{\mathbf{T}}$ and reflection $\check{\mathbf{R}}$ amplitudes from Eq. (4).

The set of closed-channel Kantorovich self-adjoint equations has the form

$$\left[-\frac{1}{\rho}\frac{d}{d\rho}\rho\frac{d}{d\rho} + \frac{\varepsilon_i(\rho)}{\rho^2} - E\right]\chi_{ii_o}(\rho) + \sum_{j=1}^{j_{\max}} W_{ij}(\rho)\chi_{ji_o}(\rho) = 0. \tag{24}$$

where the potential matrix operator $W_{ij}(\rho)$ has the form

$$W_{ij}(\rho) = V^b_{ij}(\rho) + H_{ji}(\rho) + \frac{1}{\rho}\frac{d}{d\rho}\rho Q_{ji}(\rho) + Q_{ji}(\rho)\frac{d}{d\rho}. \tag{25}$$

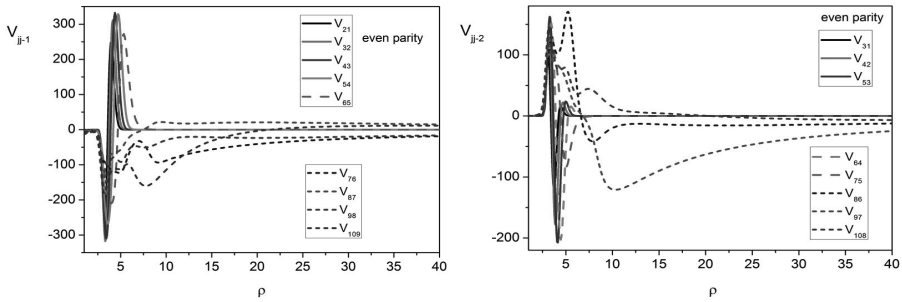

Fig. 8. Even effective potentials $V_{ij}(\rho)$ vs ρ (Å)

The potential curves $\varepsilon_j(\rho)$ (see Fig. 5) and the effective potentials $Q_{ij}(\rho) = -Q_{ji}(\rho)$, $H_{ij}(\rho) = H_{ji}(\rho)$ and $V^b_{ij}(\rho)$ (see Figs. 6–8) are determined by the integrals calculated using the program ODPEVP

$$Q_{ij}(\rho) = -\int_0^\pi d\varphi \phi_i(\varphi;\rho)\frac{d\phi_j(\varphi;\rho)}{d\rho}, H_{ij}(\rho) = \int_0^\pi d\varphi \frac{d\phi_i(\varphi;\rho)}{d\rho}\frac{d\phi_j(\varphi;\rho)}{d\rho}, \quad (26)$$

$$V^b_{ij}(\rho) = \int_0^\pi d\varphi \phi_i(\varphi;\rho)(V^b(\rho\frac{\sin(\varphi+\pi/4)}{\sqrt{2}}) + V^b(\rho\frac{\sin(\varphi-\pi/4)}{\sqrt{2}}))\phi_j(\varphi;\rho).$$

If we take the potential $V^b(\rho,\phi)$ in Eq. (21) into account by using the matrix elements $V^b_{ij}(\rho)$ from Eq.(26), then we put $V^b_{ij}(\rho) = 0$ in Eq.(25). Thus, the scattering problem for Eq. (16) with the asymptotic boundary conditions (19) is reduced to the boundary-value problem for the set of close-coupling equations in the Kantorovich form (18) with the boundary conditions at $\rho = \rho_{\min}$ and $\rho = \rho_{\max}$ [6]:

$$\left.\frac{d\boldsymbol{F}(\rho)}{d\rho}\right|_{\rho=\rho_t} = (\mathcal{R}(\rho_t) + \mathbf{Q}(\rho_t))\boldsymbol{F}(\rho_t),\ t = \min, \max, \quad (27)$$

where $\mathcal{R}(\rho)$ is an unknown $j_{\max} \times j_{\max}$ symmetric matrix function, $\boldsymbol{F}(\rho) = \{\boldsymbol{\chi}_{i_o}(\rho)\}_{i_o=1}^{N_o} = \{\{\chi_{ji_o}(\rho)\}_{j=1}^{j_{\max}}\}_{i_o=1}^{N_o}$ is the required $j_{\max} \times N_o$ matrix solution, and N_o is the number of open channels, $N_o = \max\limits_{E\geq\varepsilon_j} j \leq j_{\max}$, calculated using the program KANTBP 3.0 [3].

4 Asymptotic Form of Effective Potentials and Solutions

Algorithm 1. At large ρ, the width of the potential well is decreasing with increasing ρ (see Fig. 3). This allows linearization of the argument $\rho\sin\varphi - \hat{x}_{eq} \to \rho(\varphi - \arcsin(\hat{x}_{eq}/\rho))$ at $|x-\hat{x}_{eq}|/\rho \ll 1$ in the expression of the potential function $V^M(\rho\sin\varphi)$ and reformulation of Eq. (21) on the interval $\varphi = (0,\pi)$

$$\left(-\frac{\partial^2}{\partial\varphi^2} + \rho^2 V^M(\rho(\varphi - \arcsin(\hat{x}_{eq}/\rho))) - \varepsilon_j(\rho)\right)\phi_j(\varphi;\rho) = 0. \quad (28)$$

Table 1. The calculated coefficients $Q_{ij}^{(1)}$ $H_{ij}^{(2)}$ of expansions (31) (up rows) and corresponding numerical values Q_{ij} and H_{ij} at $\rho = 100$(down rows)

$Q_{ij}^{(1)}$ Q_{ij}	1	2	3	4	5
1	0	55.852657	–20.662584	9.913235	–4.888752
	0	0.55 863277	–0.20 664572	0.09 914008	–0.04 891971
2	–55.852657	0	66.253422	–30.004416	14.557626
	–0.55 863277	0	0.66 270932	–0.30 010937	0.14 568965
3	20.662584	–66.253422	0	62.290358	–28.724086
	0.20 664572	–0.66 270932	0	0.62 317875	–0.28 751980
4	–9.913235	30.004416	62.290358	0	43.265811
	–0.09 914008	0.30 010937	0.62 317875	0	0.43 320993
5	4.888752	–14.557626	28.724086	–43.265811	0
	0.04 891971	–0.14 568966	0.28 751983	–0.43 321006	0
$H_{ij}^{(2)}$ H_{ij}	1	2	3	4	5
1	692.635	–364.132	–462.085	397.196	–240.775
	0.0692 859	–0.0364 209	–0.0462 371	0.0397 441	–0.0241 084
2	–364.132	1718.621	–873.970	–219.292	253.669
	–0.0364 209	0.1719 273	–0.0874 195	–0.0219 721	0.0254 209
3	–462.085	–873.970	2210.843	–1250.672	244.905
	–0.0462 371	–0.0874 195	0.2211 927	–0.1251 191	0.0244 755
4	397.196	–219.292	–1250.672	2088.603	–1167.908
	0.0397 441	–0.0219 721	–0.1251 191	0.2090 243	–0.1169 414
5	–240.775	253.669	244.905	–1167.908	1209.648
	–0.0241 084	0.0254 209	0.0244 755	–0.1169 414	0.1212 568

This equation coincides with Eq. (6), (11), taking the notations

$$\hat{D} \to \hat{D}\rho^2, \hat{\rho} \to \hat{\rho}\rho, \hat{x}_{eq} \to \arcsin(\hat{x}_{eq}/\rho) \tag{29}$$

into account.

As a result, we obtain the approximate eigenvalues $\varepsilon_j(\rho)$ that depend on ρ as a parameter, expressed as

$$\varepsilon_j(\rho) = \rho^2 \varepsilon_j^{(0)}, \quad \varepsilon_j^{(0)} = -\hat{D}\left[1 - \frac{\hat{\rho}(j-\frac{1}{2})}{\sqrt{\hat{D}}}\right]^2, \quad j = 1, ..., n = \left[\frac{\sqrt{\hat{D}}}{\hat{\rho}} + \frac{1}{2}\right]. \tag{30}$$

These eigenvalues demonstrate correct asymptotic behavior $\tilde{\varepsilon}_j(\rho)/\rho^2 = \tilde{\varepsilon}_j$ describing the lower part of the discrete spectrum of problem (3). In the considered case, they correspond to the first five ($n = 5$) eigenvalues $\tilde{\varepsilon}_1, ..., \tilde{\varepsilon}_5$. The corresponding eigenfunctions $\phi_j(\varphi; \rho)$ at $j = 1, ..., n$, parametrically depending

on the slow variable ρ via the new independent variable $\zeta = \zeta(\varphi;\rho) = 2\rho\sqrt{\hat{D}}\exp[-\hat{\rho}\rho(\varphi - \arcsin(\hat{x}_{eq}/\rho))]/\hat{\rho}$, $\zeta \in [0,+\infty)$ have the form

$$\tilde{\phi}_j(\zeta;\rho) = N_j(\rho)\exp(-\frac{\zeta}{2})\zeta^{s_j}{}_1F_1(1-j,2s_j+1,\zeta),$$
$$N_j^2(\rho) = \frac{\rho\hat{\rho}\Gamma(2s_j+j)}{(j-1)!\Gamma(2s_j)\Gamma(2s_j+1)},$$

where $s_j = \sqrt{\hat{D}}/\hat{\rho} - j + 1/2$ is a positive parameter. In the considered case, the wave function outside the well at $|x - \hat{x}_{eq}|/\rho \gg 1$ is exponentially decreasing. This makes it possible to integrate the product of functions $\tilde{\psi}_j(\zeta(\varphi;\rho);\rho)$ and/or $\partial\tilde{\psi}_j(\zeta(\varphi;\rho);\rho)/\partial\rho|_{\phi=const}$ by ζ in the interval $\zeta \in (0,+\infty)$. The calculated eigenfunctions with $\rho = 10$ for $j = 1,...,5$ shown in Fig. 4 qualitatively agree with the bound states in Fig. 2. The matrix elements between the states of the lower part of the discrete spectrum $i,j = 1,...,n = 5$ with the eigenvalues $\varepsilon_j(\rho)/\rho^2 = \varepsilon_j^{(0)}$ are expanded in inverse powers of ρ:

$$Q_{ij}(\rho) = \sum_{k=1}^{k_{\max}} \frac{Q_{ij}^{(2k-1)}}{\rho^{2k-1}},\ H_{ij}(\rho) = \sum_{k=1}^{k_{\max}} \frac{H_{ij}^{(2k)}}{\rho^{2k}},\ V_{ij}(\rho) = O(\exp(-\rho)), \quad (31)$$

and calculated up to the desired order $k_{\max}$ in CAS MAPLE. As an example, the calculated coefficients $Q_{ij}^{(1)}$ and $H_{ij}^{(2)}$ of expansions (31) are presented in Table 1. For comparison, the numerical values of matrix elements Q_{ij} and H_{ij} at $\rho = 100$ are also given in Table 1. One can see that with the first nonzero coefficients of these expansions, one gets the numerical approximation of the matrix elements with three significant digits.

For the states $i,j = n+1,...,j_{\max}$ with the eigenvalues $\varepsilon_j(\rho\to\infty) = (j-n)^2 + O(1/\rho) = \varepsilon^{(2)} + O(1/\rho) = k^2 + O(1/\rho)$ corresponding to pseudo states of the BVP (6), (7) we consider the approximation by the eigenfunctions of continuous spectrum (see Eq. (14) with the notations (29)) reduced to the finite interval $\varphi \in (0,\pi/2)$ by means of the procedure implemented in CAS MAPLE. The energy spectrum of even and odd states is evaluated basing on the conditions

$$\frac{d\tilde{\phi}_k(\varphi;\rho)}{d\varphi}\Big|_{\varphi=\pi/2} = 0 \text{ and } \tilde{\phi}_k(\pi/2;\rho) = 0$$

for even and odd states, respectively. The calculated eigenfunctions at $\rho = 10$ for $i = 6,...,10$ are in quantitative agreement with the numerical ones shown in Fig. 4 and in qualitative agreement with pseudo-states displayed in Fig. 2. Thus, the basis eigenfunctions of Galerkin expansion (5) correspond to the asymptotic ones for Kantorovich expansion (20) at large values of the parameter ρ.

The diagonal and nondiagonal barrier matrix elements $V_{ij}(\rho)$ shown in Figs. 5 and 8 should be compared with the corresponding ones displayed in Fig. 2. From this comparison, one can see that the matrix elements $V_{ij}(\rho)$ from (26) between discrete-spectrum states of BVP (21), (22) and the matrix elements

$V_{ij}(y)$ from (10) between a discrete spectrum state and a pseudo-state (6), (7) demonstrate qualitatively similar behavior in the coordinates y and ρ. Since $\rho = \sqrt{x^2+y^2} > y$, the potentials $V_{ij}(\rho)$ are delocalized with respect to $V_{ij}(y)$. Due to slowly decreasing kinematic behavior of the potentials $Q_{ij}(\rho)$ and $H_{ij}(\rho)$ as ρ^{-1} and ρ^{-2}, respectively, compared to the exponentially decreasing $V_{ij}(y)$, one should take into account the leading terms of their asymptotic expressions in solving the BVP (24)-(26) generated by the Kantorovich expansion (18) in the calculation of scattering with five open channels.

Algorithm 2. Evaluation of the Asymptotic Solutions

Input. We calculate the asymptotic solution of the set of N ODEs at high values of the independent variable $\rho \gg 1$

$$\left[-\frac{1}{\rho}\frac{d}{d\rho}\rho\frac{d}{d\rho} + \frac{\varepsilon_i(\rho)}{\rho^2} + \mathcal{H}_{ii}(\rho) - 2E\right]\chi_{ii'}(\rho) \tag{32}$$
$$= \sum_{j=1,j\neq i}^{N}\left[-Q_{ij}(\rho)\frac{d}{d\rho} - \frac{1}{\rho}\frac{d}{d\rho}\rho Q_{ij}(\rho) - \mathcal{H}_{ij}(\rho)\right]\chi_{ji'}(\rho).$$

The coefficients of Eqs. (32), where $\mathcal{H}_{ij} = V^b_{ij} + H_{ij}$ are presented in the form of the inverse power series (31). In particular, $\varepsilon_i(\rho)/\rho^2 = \varepsilon_i^{(0)} + \varepsilon_i^{(2)}/\rho^2$.

Step 1. We construct the solution of Eqs. (32) in the form:

$$\chi_{ji'}(\rho) = \left(\phi_{ji'}(\rho) + \psi_{ji'}(\rho)\frac{d}{d\rho}\right)R_{i'}(\rho), \tag{33}$$

where $\phi_{ji'}(\rho)$ and $\psi_{ji'}(\rho)$ are unknown functions, $R_{i'}(\rho)$ is a known function. We choose $R_{i'}(\rho)$ as solutions of the auxiliary problem treated like an etalon equation:

$$\left[-\frac{1}{\rho}\frac{d}{d\rho}\rho\frac{d}{d\rho} + \frac{Z^{(2)}_{i'}}{\rho^2} - p^2_{i'}\right]R_{i'}(\rho) = 0, \tag{34}$$

where $Z^{(2)}_{i'} = \varepsilon^{(2)}_{i'}$.

Step 2. At this step, we compute the coefficients $\phi_{i'}(\rho)$ and $\psi_{i'}(\rho)$ of the expansion (33) in the form of truncated expansion in inverse powers of ρ ($\phi^{(k'<0)}_{ji'} = \psi^{(k'<0)}_{ji'} = 0$):

$$\phi_{ji'}(\rho) = \phi^{(0)}_{ji'} + \sum_{k'=1}^{k_{\max}}\frac{\phi^{(k')}_{ji'}}{\rho^{k'}}, \quad \psi_{ji'}(\rho) = \psi^{(0)}_{ji'} + \sum_{k'=1}^{k_{\max}}\frac{\psi^{(k')}_{ji'}}{\rho^{k'}}. \tag{35}$$

After the substitution of Eqs.(33)–(35) into Eq. (32) with the use of Eq.(34), we arrive at the set of recurrence relations at $k' \leq k_{\max}$:

$$\left(\varepsilon^{(0)}_i - 2E + p^2_{i'}\right)\phi^{(k')}_{ii'} - 2p^2_{i'}(k'-1)\psi^{(k'-1)}_{ii'} = -f^{(k')}_{ii'}, \tag{36}$$
$$\left(\varepsilon^{(0)}_i - 2E + p^2_{i'}\right)\psi^{(k')}_{ii'} + 2(k'-1)\phi^{(k'-1)}_{ii'} = -g^{(k')}_{ii'},$$

where the right-hand sides $f_{ii'}^{(k)}$ and $g_{ii'}^{(k)}$ are defined by the relations

$$
\begin{aligned}
f_{ii'}^{(k')} &= (-(k'-2)^2 - Z_{i'}^{(2)})\phi_{ii'}^{(k'-2)} + \sum_{k=2}^{k'} \mathcal{H}_{ii}^{(k)} \phi_{ii'}^{(k'-k)} \\
&+ Z_{i'}^{(2)}(2k'-4)\psi_{ii'}^{(k'-3)} + \sum_{k=1}^{k'} \sum_{j=1, j\neq i}^{N} \Big(2Q_{ij}^{(k)} Z_{i'}^{(2)} \psi_{ji'}^{(k'-k-2)} \\
&- 2p_{i'}^2 Q_{ij}^{(k)} \psi_{ji'}^{(k'-k)} + Q_{ij}^{(k)}(-2k'+k+3)\phi_{ji'}^{(k'-k-1)} + \mathcal{H}_{ij}^{(k)} \phi_{ji'}^{(k'-k)} \Big); \qquad (37) \\
g_{ii'}^{(k)} &= (-(k'-1)^2 - Z_{i'}^{(2)})\psi_{ii'}^{(k'-2)} + \sum_{k=2}^{k'} \mathcal{H}_{ii}^{(k)} \psi_{ii'}^{(k'-k)} \\
&+ \sum_{j=1, j\neq i}^{N} \sum_{k=1}^{k'} \Big(2Q_{ij}^{(k)} \phi_{ji'}^{(k'-k)} - Q_{ij}^{(k)}(2k'-1-k)\psi_{ji'}^{(k'-k-1)} + \mathcal{H}_{ij}^{(k)} \psi_{ji'}^{(k'-k)} \Big)
\end{aligned}
$$

with the initial conditions $p_{i'}^2 = 2E - \varepsilon_{i'}^{(0)}$, $\phi_{ii'}^{(0)} = \delta_{ii'}$, $\psi_{ii'}^{(0)} = 0$.

Step 3. Here we calculate the coefficients $\phi_{ii'}^{(k')}$ and $\psi_{ii'}^{(k')}$ using the step-by-step procedure of solving Eqs. (36) for $2E \neq \epsilon_{i'}^{(0)}$, $i \neq i'$ and $k' = 2, \ldots, k_{\max}$:

$$
\begin{aligned}
\phi_{ii'}^{(k')} &= \left[\varepsilon_i^{(0)} - \varepsilon_{i'}^{(0)}\right]^{-1} \left[-f_{ii'}^{(k')} + 2p_{i'}^2(k'-1)\psi_{ii'}^{(k'-1)}\right], \\
\psi_{ii'}^{(k')} &= \left[\varepsilon_i^{(0)} - \varepsilon_{i'}^{(0)}\right]^{-1} \left[-g_{ii'}^{(k')} - 2(k'-1)\phi_{ii'}^{(k'-1)}\right], \\
\phi_{i'i'}^{(k'-1)} &= -\left[2(k'-1)\right]^{-1} g_{i'i'}^{(k)}, \qquad (38) \\
\psi_{i'i'}^{(k'-1)} &= \left[2(k'-1)\left(2E - \varepsilon_{i'}^{(0)}\right)\right]^{-1} f_{i'i'}^{(k)}.
\end{aligned}
$$

The above described algorithm was implemented in MAPLE and FORTRAN to calculate the desired $\phi_{ii'}^{(k')}$ and $\psi_{ii'}^{(k')}$ in the **output** up to needed order of $k_{\max}$.

The choice of appropriate values $\rho_{\min}$ and $\rho_{\max}$ for the constructed expansions of the linearly independent solutions for $p_{i_o} > 0$ is controlled by the fulfilment of the Wronskian condition to the prescribed precision ε_{Wr}:

$$
\begin{aligned}
&Wr(\mathbf{Q}(\rho); \boldsymbol{\chi}^*(\rho), \boldsymbol{\chi}(\rho)) = \frac{2\imath}{\pi} \mathbf{I}_{oo}, \qquad (39) \\
&W(\mathbf{Q}, \boldsymbol{\chi}^*, \boldsymbol{\chi}) \equiv \rho \left(\boldsymbol{\chi}^{*T} \left(\frac{d\boldsymbol{\chi}}{d\rho} - \mathbf{Q}\boldsymbol{\chi} \right) - \boldsymbol{\chi}^T \left(\frac{d\boldsymbol{\chi}^*}{d\rho} - \mathbf{Q}\boldsymbol{\chi}^* \right) \right).
\end{aligned}
$$

5 Analysis of Quantum Tunneling Problem

The solutions of the BVPs (8)–(15) and (24)–(27) were performed on the finite-element grids $\Omega_y = \{-12(N_{elem} = 120)12\}$ and $\Omega_\rho = \{0(N_{elem} = 1200)120\}$, respectively, with N_{elem} fourth-order Lagrange elements $p = 4$ between the

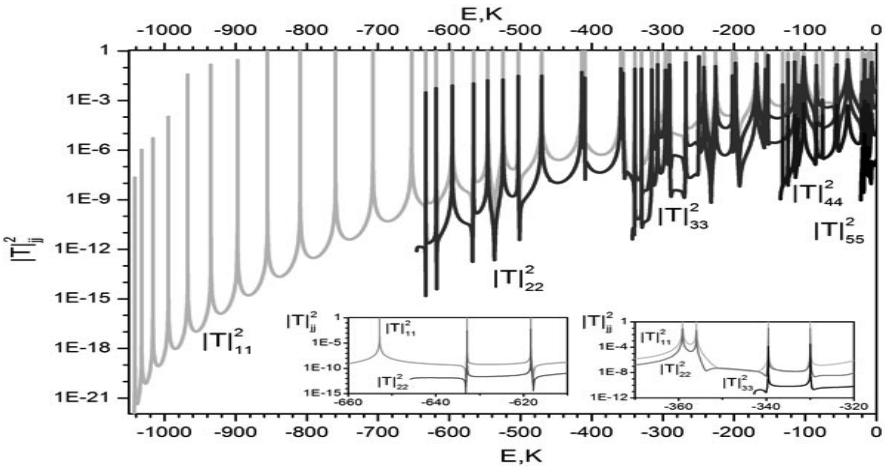

Fig. 9. The total probability of penetration from the first channels with the energies $E_1 = -1044.879649$, $E_2 = -646.1570935$, $E_3 = -342.7919791$, $E_4 = -134.7843058$, $E_5 = -22.13407384$ (in K) to all five open channels simulated by the Galerkin and Kantorovich expansions

nodes using the program KANTBP 3.0. The expansion of the desirable solution (5) over such orthogonal basis at ($j_{max} = 15$) with only ten closed channels taken into account allows the calculation of approximate solutions of the original 2D problem (1) at $E < 0$ with the required accuracy. Fig. 9 shows the resonance behavior of the total penetration probability with the transition from the first channels having the energies $E_1 = -1044.879649$, $E_2 = -646.1570935$, $E_3 = -342.7919791$, $E_4 = -134.7843058$, $E_5 = -22.13407384$ (in K) to all five open channels, simulated using the Galerkin expansion (5) as well as the Katorovich one (18). The total transmission probability is seen to demonstrate the resonance behavior, i.e., effect of quantum transparency. Some peaks are high and narrow, and the positions of peaks corresponding to transitions from different bound states are similar.

As the energy of the initial excited state increases, the transmission peaks demonstrate a shift towards higher energies, the set of peak positions keeping approximately the same as for the transitions from the ground state and the peaks just replacing each other. For example, the left epure shows that the positions of the 13th and 14th peaks for transitions from the first state coincide with the positions of the 1st and 2nd peaks for the transitions from the second state, while the right epure shows that the positions of the 25th and 26th peaks for transitions from the first state coincide with the positions of the 13th and 14th peaks for transitions from the second state and with the positions of the 1st and 2nd peaks for the transitions from the third state.

As one can see from Fig. 2, the diagonal matrix elements of the potential $V^b_{jj}(y)$ have the shapes of double barriers, and the nondiagonal matrix elements

$V_{ij}^b(y)$ are by more than four times smaller than $V_{jj}^b(\rho)$ and $V_{ij}^b(\rho)$ in Figs. 5 and 8. It means that the position of peaks corresponds to the real part of energy of the metastable states embedded in the continuum, which are mainly localized between double barriers.

6 Conclusions

We have demonstrated efficiency of symbolic-numeric algorithms for solving the boundary-value problems that describe the quantum tunneling of diatomic low-dimensional model systems, coupled via realistic molecular potentials, through repulsive barriers below a dissociation threshold. We presented a comparative analysis of the potential matrix elements and solutions with different asymptotic behavior calculated in the Cartesian and polar coordinates. The necessity for two statements of the problem follows from the important practical applications of further self-consistent study of the system above the dissociation threshold, which is convenient in polar coordinates. The effect of quantum transparency in resonance tunneling of diatomic molecules through repulsive potential barriers was revealed that produced by metastable states imbedded in continuum. The proposed models and elaborated symbolic-numerical algorithms, the quantum transparency effect itself, and the developed software can find further applications in barrier heavy-ion reactions and molecular quantum diffusion. The authors thank Prof. F.M. Penkov for collaboration. The work was supported partially by grants RFBR 14-01-00420 and 13-01-00668 and 0602/GF MES RK.

References

1. Bondar, D.I., Liu, W.-K., Ivanov, M.Y.: Enhancement and suppression of tunneling by controlling symmetries of a potential barrier. Phys. Rev. A 82, 052112–1–9 (2010)
2. Chuluunbaatar, O., Gusev, A.A., Derbov, V.L., Kaschiev, M.S., Melnikov, L.A., Serov, V.V., Vinitsky, S.I.: Calculation of a hydrogen atom photoionization in a strong magnetic field by using the angular oblate spheroidal functions. J. Phys. A 40, 11485–11524 (2007)
3. Chuluunbaatar, O., Gusev, A.A., Vinitsky, S.I., Abrashkevich, A.G.: KANTBP 2.0: New version of a program for computing energy levels, reaction matrix and radial wave functions in the coupled-channel hyperspherical adiabatic approach. Comput. Phys. Commun. 179, 685–693 (2008)
4. Chuluunbaatar, O., Gusev, A.A., Vinitsky, S.I., Abrashkevich, A.G.: ODPEVP: A program for computing eigenvalues and eigenfunctions and their first derivatives with respect to the parameter of the parametric self-adjoined Sturm-Liouville problem. Comput. Phys. Commun. 180, 1358–1375 (2009)
5. Fundamental Physical Constants, `http://physics.nist.gov/constants`
6. Gusev, A.A., Vinitsky, S.I., Chuluunbaatar, O., Gerdt, V.P., Rostovtsev, V.A.: Symbolic-numerical algorithms to solve the quantum tunneling problem for a coupled pair of ions. In: Gerdt, V.P., Koepf, W., Mayr, E.W., Vorozhtsov, E.V. (eds.) CASC 2011. LNCS, vol. 6885, pp. 175–191. Springer, Heidelberg (2011)

7. Vinitsky, S., Gusev, A., Chuluunbaatar, O., Rostovtsev, V., Le Hai, L., Derbov, V., Krassovitskiy, P.: Symbolic-numerical algorithm for generating cluster eigenfunctions: tunneling of clusters through repulsive barriers. In: Gerdt, V.P., Koepf, W., Mayr, E.W., Vorozhtsov, E.V. (eds.) CASC 2013. LNCS, vol. 8136, pp. 427–442. Springer, Heidelberg (2013)
8. Kavka, J.J., Shegelski, M.R.A., Hong, W.P.: Tunneling and reflection of an exciton incident upon a quantum heterostructure barrier. J. Phys.: Condens. Matter. 24, 365802–1–13 (2012)
9. Lauhon, L.J., Ho, W.: Direct observation of the quantum tunneling of single hydrogen atoms with a scanning tunneling microscope. Phys. Rev. Lett. 85, 4566–4569 (2000)
10. Pen'kov, F.M.: Metastable states of a coupled pair on a repulsive barrier. Phys. Rev. A 62, 044701–1–4 (2000)
11. Pen'kov, F.M.: Quantum transmittance of barriers for composite particles. JETP 91, 698–705 (2000)
12. Pijper, E., Fasolino, A.: Quantum surface diffusion of vibrationally excited molecular dimers. J. Chem. Phys. 126, 014708–1–10 (2007)
13. Shegelski, M.R.A., Hnybida, J., Vogt, R.: Formation of a molecule by atoms incident upon an external potential. Phys. Rev. A. 78, 062703–1–5 (2007)